

ON THE RECONSTRUCTION PERFORMANCE OF COMPRESSED ORTHOGONAL MOMENTS

G.A.Papakostas, Y.S.Boutalis

Democritus University of Thrace, Department of Electrical and Computer Engineering, 67100 Xanthi, Greece
Email: gpapakos@ee.duth.gr,ybout@ee.duth.gr

D.A.Karras

Hellenic Aerospace Industry and University of Herfordshire, Rodu 2, Ano Iliupolis, 16342 Athens, Greece
Email: dakarras@usa.net

B.G.Mertzios

Thessaloniki Institute of Technology, Department of Automation, Laboratory of Control Systems and Comp.Intelligence
Email: mertzios@uom.gr

Keywords: Zernike, Pseudo-Zernike, Fourier-Mellin, orthogonal moments, wavelet compression, image reconstruction

Abstract: In this paper, a wavelet-based technique is applied to three moment feature vectors corresponding to three different families of orthogonal moments. The resulted compressed vectors are studied experimentally, in order to extract useful information about their behaviour to a reconstruction procedure. The reconstruction performance of these moments is identical to the amount of image information that they contain to certain moment orders. Since the moment vectors are imposed to compression at the high frequency components, a conclusion about their information redundancy can be also determined. The most efficient moment family, by means of the reconstruction error, will form feature vectors with low dimension, yet with high information content and thus will be very useful for pattern recognition applications, guarantying high recognition rates.

1 INTRODUCTION

Image moments have played a major role in vision systems, since their first introduction by Hu (Hu, 1962). They have been used as image descriptors, able to characterize an image uniquely. The uniqueness property unfortunately is satisfied only by the orthogonal moments, which derived from orthogonal polynomials consisting an orthonormal basis. This feature makes them more useful than the conventional ones, since they guarantee a small information redundancy and high reconstruction capabilities.

In general an infinite number of moments can describe the whole image, but in practical applications a finite number of them is mostly needed. Thus, there is a need to use the appropriate moment feature vector that encloses as much as possible image information. By applying a compression method to the moment feature vector,

this requirement is satisfied (Papakostas, 2002, 2004).

In this paper, an investigation about the reconstruction performance of three popular families of orthogonal moments, which have been processed by using the above procedure, is attempted. The present study is focused on the reconstruction capability of the three compressed moment vectors; in order to decide which orthogonal moment family behaves appropriately, by means of the image reconstruction error.

The most efficient moment family, which will be obtained, can be used in any pattern recognition task, as a discriminative feature vector, as it has already been presented in (Papakostas, 2004).

The following sections, are introducing the Zernike moments (ZMs), Pseudo-Zernike moments (PZMs) and Fourier-Mellin orthogonal moments (OFMMs), and the processing algorithm that these moments will be imposed to. Finally, in the last section, an experimental study is taking place in

order to justify the performance of each orthogonal moment family, in reconstructing an image by using as small as possible moment features.

2 ORTHOGONAL MOMENTS

Orthogonal moments have been proved a major image descriptor, as feature vectors, in many pattern recognition tasks. Their ability to describe an image fully, with minimum information redundancy, due to their orthogonality property, as well as their robustness in noisy environments, have established them as the most efficient among the moment descriptors.

The present paper, investigates the reconstruction performance, of the three most powerful orthogonal moments the Zernike, Pseudo-Zernike and Fourier-Mellin moments, that have been affected by a wavelet based compression method.

Their performance is being compared to that of the uncompressed moments of the same family. Also, by comparing the performance of these families, a conclusion about the most efficient, in the sense of their reconstruction error, is being derived.

2.1 Zernike Moments

Zernike introduced a set of complex polynomials, which form a complete orthogonal set over the interior of the unit circle $x^2+y^2=1$. These polynomials (Khotanzad, 1990) have the form

$$V_{pq}(x, y) = V_{pq}(r, \theta) = R_{pq}(r) \exp(jq\theta) \quad (1)$$

where p is non-negative integer, q is a non zero integer subject to constraints (i) $p-|q|$ being even, (ii) $|q| \leq p$, r is the length of vector from origin (x, y) to pixel with coordinates (x, y) , θ the angle between vector r and x axis in counter-clockwise direction, $R_{pq}(r)$ are the Zernike radial polynomials in (r, θ) polar coordinates defined as

$$R_{pq}(r) = \sum_{s=0}^{p-|q|/2} (-1)^s \cdot \frac{(p-s)!}{s! \left(\frac{p+|q|}{2} - s\right)! \left(\frac{p-|q|}{2} - s\right)!} r^{p-2s} \quad (2)$$

Note that $R_{p,-q}(r) = R_{pq}(r)$

Zernike moment of order p with repetition q , for a digital image with intensity function $f(x, y)$, that vanishes outside the unit disk is

$$Z_{pq} = \frac{p+1}{\pi} \sum_x \sum_y f(x, y) V_{pq}^*(r, \theta), \quad x^2 + y^2 \leq 1 \quad (3)$$

The rotation invariant property of ZMs has been already studied (Khotanzad, 1990). These investigations led to the conclusion that the magnitudes of ZMs are invariant to any rotation of the image. Thus, the magnitudes of the resulted ZMs beyond a high order can be used for our experiments.

According to (2) there are a lot of computations (factorials) that should be taken into account, in order to calculate the radial polynomials. For this reason many researchers have introduced methods for fast computation of ZMs (Mukundan, 1995). Among these, there is an efficient one (Chong, 2003) the well-known “q-recursive method”. This method permits the evaluation of radial polynomials by using the following recursive equations,

- for $p=q$

$$R_{pq}(r) = r^p \quad (4)$$

- for $p-q=2$

$$R_{p(p-2)}(r) = pR_{pp}(r) - (p-1)R_{(p-2)(p-2)}(r) \quad (5)$$

- otherwise

$$R_{p(q-4)}(r) = H_1 R_{pq}(r) + (H_2 + \frac{H_3}{r^2}) R_{p(q-2)}(r) \quad (6)$$

where the coefficients H_1 , H_2 and H_3 are given by

$$\begin{aligned} H_1 &= \frac{q(q-1)}{2} - qH_2 + \frac{H_3(p+q+2)(p-q)}{8} \\ H_2 &= \frac{H_3(p+q)(p-q+2)}{4(q-1)} + (q-2) \\ H_3 &= -\frac{-4(q-2)(q-3)}{(p+q-2)(p-q+4)} \end{aligned} \quad (7)$$

The original image can be reconstructed using a finite number of ZMs, by applying the following inverse formula

$$\hat{f}(r, \theta) = \sum_{p=0}^{p_{\max}} \sum_{q} Z_{pq} V_{pq}(r, \theta) \quad (8)$$

2.2 Pseudo-Zernike Moments

Pseudo-Zernike moments are used in many pattern recognition applications as alternatives to the traditional ZMs. It has been proved that they have better feature representation capabilities and are more robust to image noise (Teh, 1988) than the last ones.

The kernel of these moments is the orthogonal set of Pseudo-Zernike polynomials defined inside the unit circle. These polynomials have the form of (1) with the Zernike radial polynomials replaced by the Pseudo-Zernike radial polynomials

$$S_{pq}(r) = \sum_{s=0}^{p-|q|} (-1)^s \cdot \frac{(2p+1-s)!}{s!(p+|q|+1-s)!(p-|q|-s)!} r^{p-s} \quad (9)$$

with additional constraints

$$0 \leq |q| \leq p, \quad p = 0, 1, 2, \dots, \infty \quad (10)$$

The corresponding PZMs are computed using the same formula (2) as in the case of ZMs, since the only difference is pointed only to the form of the polynomial being used.

Due to the above constraints, the set of Pseudo-Zernike polynomials of order $\leq p$, contain $(p+1)2$ linearly independent polynomials of degree $\leq p$. On the other hand the set of Zernike polynomials contain only $(p+1)(p+2)/2$ linearly independent polynomials of degree $\leq p$, due to the additional condition that $p-|q|$ is even.

Thus, PZMs offer more feature vectors than the Zernike moments of the same order.

As can be seen from equation (9) the computation of Pseudo-Zernike moments, involves the calculation of some factorial terms, an operation that adds an extra overhead. For this reason, in the present paper a recurrence relation among the Pseudo-Zernike polynomials is used, for reducing the computational time.

The method that is used is called “*two-stage recursive*” algorithm, whose detailed description can

be found in (Chong, 2001). This method makes use of the following recursive relations

- for $p=q$

$$R_{pq}(r) = r^p \quad (11)$$

- for $p-q < 2$

$$R_{p(p-1)}(r) = (2p+1)R_{pp}(r) - (2p)R_{(p-1)(p-1)}(r) \quad (12)$$

- otherwise

$$R_{pq}(r) = (L_1 r + L_2)R_{(p-1)q}(r) + L_3 R_{(p-2)q}(r) \quad (13)$$

where the coefficients $L1$, $L2$ and $L3$ are given by

$$\begin{aligned} L_1 &= \frac{(2p+1)(2p)}{(p+q+1)(p-q)} \\ L_2 &= -2p + \frac{(p+q)(p-q-1)}{2p-1} L_1 \\ L_3 &= (2p-1)(p-1) - \frac{(p+q-1)(p-q-2)}{2} L_1 + \\ &\quad 2(p-1)L_2 \end{aligned} \quad (14)$$

Similarly to ZMs, an image described by a finite number of PZMs, can be reconstructed by using equation (8).

2.3 Fourier-Mellin Moments

Fourier-Mellin moments, is the third family of orthogonal moments, that will be used in the present experiments. These orthogonal moments are based on a complete set of orthogonal polynomials defined over the unit circle and have the form

$$Q_p(r) = \sum_{s=0}^p a_{ps} r^s \quad (15)$$

where

$$a_{ps} = (-1)^{p+s} \frac{(p+s+1)!}{(p-s)!s!(s+1)!} \quad (16)$$

The corresponding orthogonal Fourier-Mellin moments (OFMMs) can be defined as

$$\Phi_{pq} = \frac{p+1}{\pi} \sum_x \sum_y f(x, y) Q_p(r) e^{-iq\theta} \quad (17)$$

where $p \geq 0$, $q = 0, \pm 1, \pm 2, \dots$

By using an infinite number of moments Φ_{pq} , $-M \leq q \leq M$, $0 \leq p \leq N$, where M, N are positive integers, the original image can be reconstructed through the following formula

$$\hat{f}(r, \theta) = \sum_{p=0}^N \sum_{q=-M}^M \Phi_{pq} Q_p e^{iq\theta} \quad (18)$$

As in the case of Zernike and Pseudo-Zernike moments, the magnitudes of the OFMMs are also rotation invariant. The majority of OFMMs in contrast to the other orthogonal moments is focused on the fact, that they can describe the high spacial frequency components of an image more accurately (Kan, 2002). This capability comes from the number of zeros of their radial polynomials, which is greater than the other moments.

The number of linearly independent OFMMs is $(p+1)^2$, so the degree p of Q_p in the OFMMs required to represent an image can be much lower than a representation using ZMs and PZMs.

Because the Zernike, Pseudo-Zernike and Fourier-Mellin moments are only rotationally invariant, additional properties of translation and scale invariance must be given to these moments in some way. We can ensure these invariances by converting the absolute pixel coordinates (Khotanzad, 1990).

3 MOMENT COMPRESSION

In this section a predefined algorithm that consists of two complementary paths, involving moment computation and a compression method, is presented.

In Fig.1 this algorithm is depicted in a generic form, in order to maintain a systematic procedure that performs a feature extraction method, while the inverse process is also provided.

The concerned algorithm, which is presented in details in (Papakostas, 2002, 2004), can be summarized in the following steps:

Direct path

- Step 1:* The original image is being pre-processed, (filtering, binarization).
- Step 2:* Computation of the orthogonal moments to be compressed, with the additional ensuring of translation, scaling invariance, and finally the computation of the so called “moment signal”. This 1-D signal consists of the

resulted moments, in the order they have been produced.

Step 3: Application of the Wavelet transform, or an alternative one (Fourier), to the “moment signal”.

Step 4: Compression by thresholding of the resulted wavelet (Fourier) coefficients.

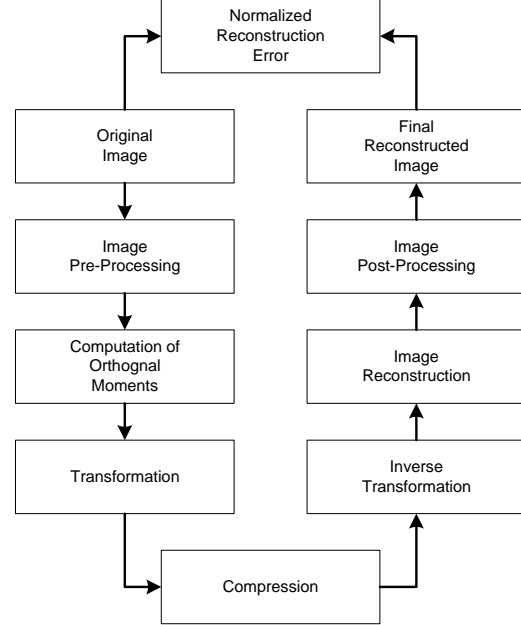


Figure 1: Generic compression of moment features.

Inverse path

Step 1: Application of the inverse transform, upon the compressed coefficients, in order to construct the compressed “moment signal”.

Step 2: Image reconstruction using the compressed moments, by applying the inverse formula of the corresponding moment family.

Step 3: Image post-processing, including mapping into the range [0-255], binarization or histogram equalization.

The direct path of the above algorithm is applied, in order to generate feature vectors with an as small as possible dimension, but with an increasing amount of image information. The resulted feature vectors are consisted of wavelet coefficients that describe the compressed moment signal.

The inverse path being used to verify the effectiveness of the moment based feature vectors, by means of the normalized reconstruction error.

In the present paper, the above direct path of the algorithm is applied to the three sets of orthogonal moments that have been already presented, and three feature vectors are obtained. The resulted feature vectors are compared to each other, by computing their respective normalized reconstruction errors, through the inverse path of the algorithm.

4 EXPERIMENTAL STUDY

In this section, the reconstruction performance of the three moment families, are presented and compared to each other.

For the present experiments, the wavelet transform is used to extract the image coefficients, which will be compressed by soft thresholding (Donoho, 1995). The binarization procedure is performed by thresholding using the Otsu method, while the reconstruction performance is measured by means of the normalized reconstruction error (Teh, 1988), defined as

$$\bar{e}^2 = \frac{\sum_{i} \sum_{j} [f(i,j) - f'(i,j)]^2}{\sum_{i} \sum_{j} [f(i,j)]^2} \quad (19)$$

where $f(i,j)$ is the intensity function of the original image and $f'(i,j)$ the intensity function of the reconstructed one.

In Figure 2, the mean normalized reconstruction error for the set of images used in (Papakostas, 2004), for each one of the families of orthogonal moments, is illustrated.

As can be seen, in the case of Zernike moments the compression method yields to a set of more efficient feature vectors, since for the same number of features the corresponding error is smaller than that of the uncompressed ones.

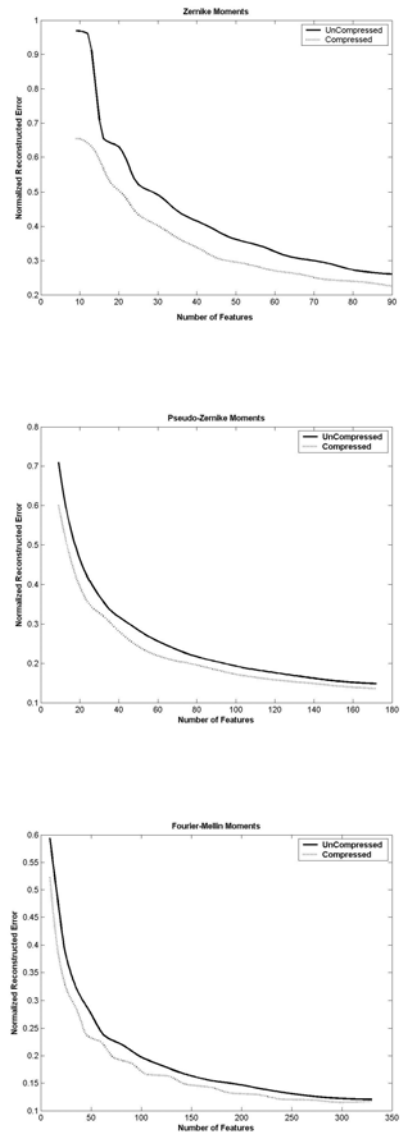


Figure 2: Uncompressed vs Compressed (a) Zernike, (b) Pseudo-Zernike and (c) Fourier-Mellin moments.

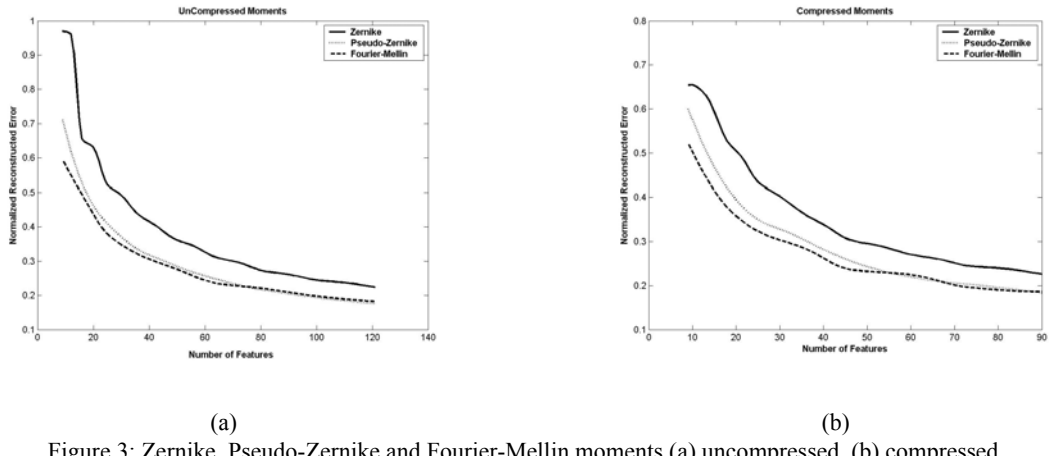


Figure 3: Zernike, Pseudo-Zernike and Fourier-Mellin moments (a) uncompressed, (b) compressed.

In a sense the “moment signals” consisted of the Zernike moments, have some kind of quantization error, appeared as noise in the high frequency bands, and the application of the compression method operates as denoising. This can be verified by the fact that Zernike moments are very sensitive to the presence of noise.

This effect is appeared in a smaller amount in Pseudo-Zernike and Fourier-Mellin moments, with the last ones being the most robust noise of all.

Additionally, Figure 2 points that the proposed algorithm can be applied successfully, in all orthogonal moments keeping the appropriate image information for the reconstruction of the initial image with minimum reconstruction error.

Finally, Figure 3 shows that the compression method improves the reconstruction ability of Fourier-Mellin moments more than the Pseudo-Zernike one.

For the above experiments some test objects (patterns) are initially selected. Figure 4b shows a wooden pyramidal puzzle, which is used for robot vision tasks in the Control Systems Lab of DUTH. The nine parts of the puzzle, placed in arbitrary positions, are shown in figure 4a. The (256x256) images of these parts are the nine patterns of our experiments.

5 CONCLUSIONS

An investigation of the performance of a compression-based algorithm, to moment signals derived from three different families of orthogonal moments, was presented in the previous sections. The performance was measured, subject to the reconstruction error that the compressed moments resulted.

Fourier-Mellin moments seem to improve their ability in representing an image by a set of compressed feature moments, better than the other two families.

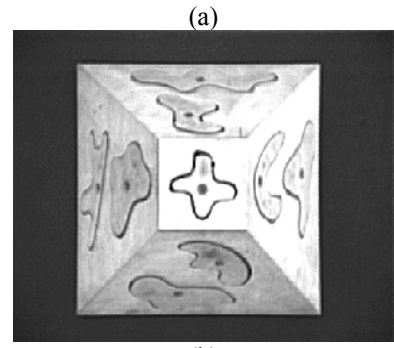
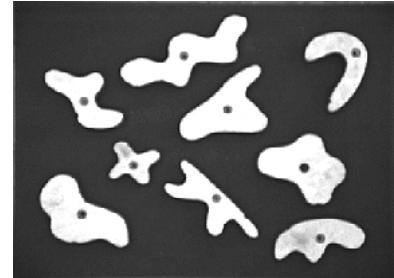


Figure 4: The nine work pieces that are placed (a) in arbitrary positions on the table and (b) on a 3-D truncated pyramid.

The performance of the compressed Pseudo-Zernike moments remains quite the same to this of the uncompressed ones, while the application of compression to the Zernike moment signal can be considered as denoising, by removing the high frequency components.

REFERENCES

Chong Chee-Way, Mukundan R., Raveendran P., 2001. "An efficient Algorithm for fast computation of Pseudo-Zernike Moments", International conference on Image and Vision Computing – (IVVCNZ'01), pp. 237-242, New Zealand.

Chong Chee-Way, Raveendran P., Mukundan R., 2003. "A comparative analysis of algorithms for fast computation of Zernike moments", Pattern Recognition 36, pp. 731-742.

Donoho D.L., 1995. "De-noising by soft-thresholding", IEEE Trans. on Inf. Theory, vol. 41, No. 3, pp. 613–627.

Hu M.K., 1962. "Visual pattern recognition by moment invariants", IRE Trans. Inform. Theory, vol. IT-8, pp. 179-187.

Kan C., Srinath M.D., 2002. "Invariant character recognition with Zernike and orthogonal Fourier-Mellin moments", Pattern Recognition 35, pp. 143-154.

Khotanzad A. and Hong Y.H., 1990. "Invariant Image Recognition by Zernike Moments", IEEE Trans. on Pattern Anal. Machine Intell., vol. PAMI-12, No.5., pp. 489-497.

Mukundan R., Ramakrishnan K.R., 1995. "Fast computation of Legendre and Zernike moments", Pattern Recognition 28 (9), pp. 1433-1442.

Papakostas G.A., Karras D.A., Mertzios B.G., 2002. "Image Coding Using a Wavelet Based Zernike Moments Compression Technique", 14th International Conference on Digital Signal Processing (DSP2002), vol. II, pp. 517-520, 1-3 July 2002, Santorini-Hellas (Greece).

Papakostas G.A., Karras D.A., Mertzios B.G. and Boutalis Y.S., 2004. "Pattern Classification by Wavelet Based Compressed Zernike Moments", submitted to EURASIP Journal of Applied Signal Processing.

Teh C.-H. and Chin R.T., 1988. "On Image Analysis by the Methods of Moments", IEEE Trans. on. Pattern Anal. Machine Intell., vol. PAMI-10, No.4. pp. 496-513.